Iris Segmentation using Gradient Magnitude and Fourier Descriptor for Multimodal Biometric Authentication System

Defiana Sulaeman[1], Anto Satriyo Nugroho[2,*] & Maulahikmah Galinium[1]

[1]Department of Information Technology, Swiss German University
Edutown BSD City, Tangerang 15339, Indonesia
[2]Center for Information and Communication Technology Agency for Assessment & Application of Technology (PTIK-BPPT)
Teknologi 3 Bld., 2F, Puspitek Serpong, Tangerang Selatan, Indonesia
*E-mail: anto.satriyo@bppt.go.id

Abstract. Perfectly segmenting the area of the iris is one of the most important steps in iris recognition. There are several problematic areas that affect the accuracy of the iris segmentation step, such as eyelids, eyelashes, glasses, pupil (due to less accurate iris segmentation), motion blur, and lighting and specular reflections. To solve these problems, gradient magnitude and Fourier descriptor are employed to do iris segmentation in the proposed Multimodal Biometric Authentication System (MBAS). This approach showed quite promising results, i.e. an accuracy rate of 97%. The result of the iris recognition system was combined with the result of an open-source fingerprint recognition system to develop a multimodal biometrics authentication system. The results of the fusion between iris and fingerprint authentication were 99% accurate. Data from Multimedia Malaysia University (MMUI) and our own prepared database, the SGU-MB-1 dataset, were used to test the accuracy of the proposed system.

Keywords: *biometrics; conditional dilation; horizontal projection; iris recognition; iris segmentation; Sobel edge detector; vertical projection.*

1 Introduction

Biometrics is one way of implementing a better security system. There are plenty of biometrics features that can be used, such as face, fingerprint, voice, handwritten signatures, retina, iris, gait, palm print, and ear and hand geometry [1]. However, among these features, the iris is known as the most reliable and stable one, because it has a random morphogenesis and apparently no genetic penetrance [2].

In a previous study, Sentanoe [3] investigated an iris segmentation module and successfully implemented a conditional dilation technique by using a gradient magnitude calculation. The results of this study were quite promising. However,

Received August 3rd,2015, 1st Revision November 2nd, 2015, Accepted for publication June, 14th, 2016.
 ISSN: 2337-5787, DOI: 10.5614/itbj.ict.res.appl.2016.10.3.2

the segmentation module still needs improvement regarding the following problems:

1. Smooth intensity transition causing the sclera region to be detected as iris region.
2. Thick eyelashes causing eyelashes to be detected as pupil region.
3. Noise in the pupil area causing failure in finding an accurate pupil and iris area.

After several inspections and analysis, it was found that these problems are caused by the misplacement of the pupil's and the iris's initial point. This misplacement of both initial points causes failure in the conditional dilation step, which is important in finding the pupil and the iris region. Therefore, the main purpose of this study was to improve the initial point localization step.

The remainder of this paper is organized as follows. Section 2 discusses related works. The proposed method is explained in Section 3. Section 4 explains the experimental results. Finally, Section 5 discusses the conclusions and future work.

2 Related Works

Daugman has proposed an integro-differential operator to localize the area of the iris and detect eyelid noise [4]. The algorithm is based on a circular edge detector and is used to obtain the maximum integral derivative value with its corresponding parameter. Then, in order to detect the eyelid occlusions, the path of the contour in the formula is changed from circular to parabolic. However, this algorithm still has problems with specular reflections in the pupil.

Ross and Shah have proposed the geodesic active contours algorithm for segmenting non-ideal irises. This algorithm belongs to the first algorithm model [5]. There are two processes involved in this algorithm, pupil segmentation and iris segmentation [5].

Abhyankar and Schuckers introduced the active shape model for segmenting the iris [6]. Instead of using rule-based reasoning for the shape modelling, this model uses a statistical learning method, which is more efficient in constraining the search [6]. The active shape model does not use any shape modelling. Instead, this model tries to search for the best landmarks and regularize the contour to the space of the training shapes.

Using Daugman's [4] research as a benchmark, Valentina has done some research regarding an iris segmentation module [7]. She used a circular Hough

transform algorithm and horizontal projection folding. The algorithm aims to find a circular object within an image. However, human irises and pupils are not perfectly circular. Therefore, this approach has difficulty in localizing the iris.

For this reason, Sentanoe [3] have tried to improved Valentina's [7] iris segmentation module by implementing the geodesic active contour algorithm as suggested by Ross and Shah [5]. Sentanoe proposed a circular gradient magnitude and Fourier descriptor algorithm to segment the iris. The purpose of this technique is to localize the iris by approximating the intensity transition from dark to light objects and vice versa. Thus, it is able to segment the iris without assuming a circular shape of the iris' outer boundary. Although the results of his iris segmentation module were quite promising, it still needs to be improved, especially in the initial point localization step.

The accuracy of the segmentation is sensitive to the initial point selection. Therefore, in this study we modified the algorithm by including a robust technique for initial point localization. Compared to Ross and Shah [5], the proposed method offers a simple conditional-dilation approach that is less computationally intensive. Our experimental results showed that the accuracy of the segmentation module was improved. We also integrated the iris segmentation module into a complete iris recognition system and combined it with an open-source fingerprint recognition system to compare the performance obtained by one single biometric trait versus a multimodal approach.

3 Proposed Method

As stated in Section 2, this research is an enhancement of our previous studies [3] and [7]. Figure 1 shows a scheme of the multimodal biometrics fusion between iris recognition and fingerprint recognition.

3.1 SGU-MB-1 Dataset Preparation

The SGU-MB-1 dataset was created during this study. This dataset consists of two pairs of iris images, two pairs of point finger fingerprint images, and two faces images of one hundred eleven staff members and students of the Swiss German University. The iris images were used to test the proposed iris segmentation module and the fingerprint images were used as input for the open-source fingerprint recognition system.

To capture the eye images, a Mobile-Eyes Iris Scanner device was used. This scanner has a USB 2.0 device connection and the illumination is near infrared. The size of the resulted images was 640 x 480 pixels. The fingerprints were captured with a Futronic FS88H Fingerprint Scanner device. This device has a

16.26 x 24.38 mm window size. The resolution of the resulted images was 320 x 480 pixels at 500 DPI.

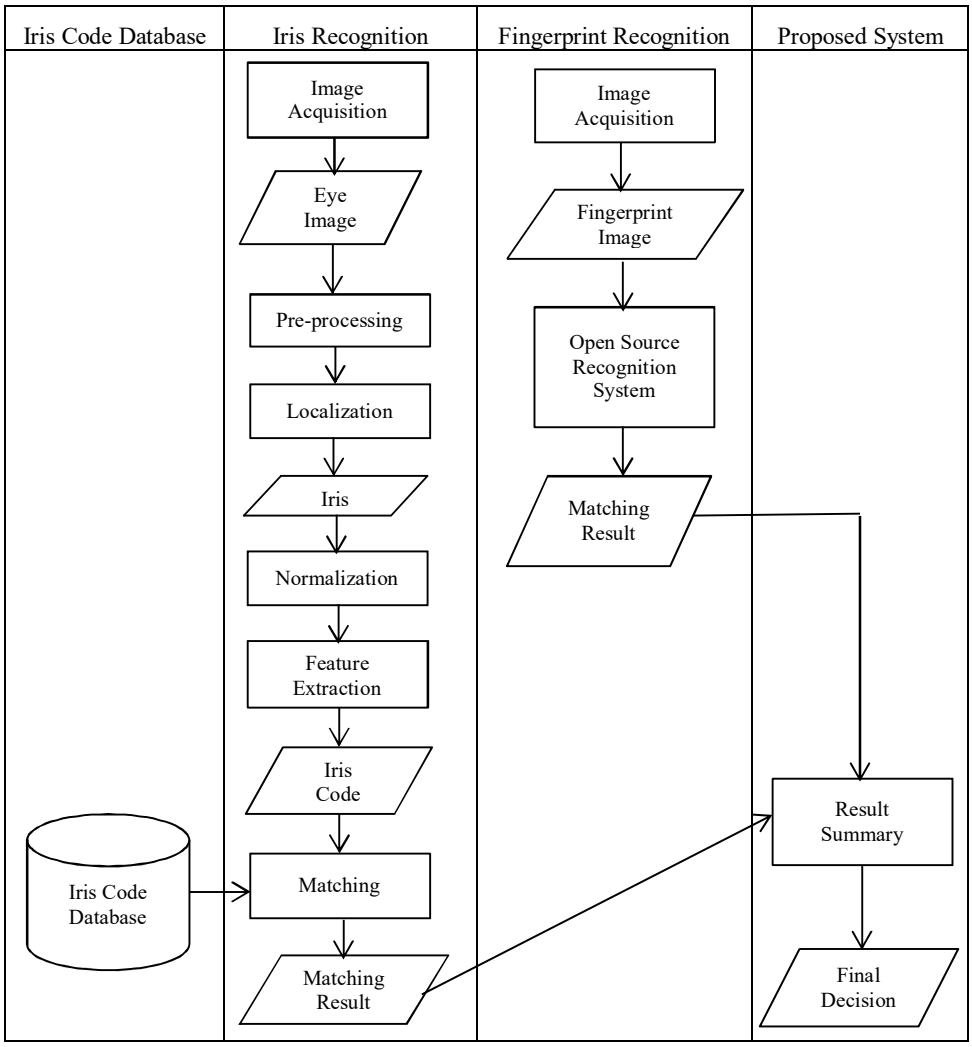

Figure 1 Activity diagram of the proposed system.

3.2 Iris Recognition

The system consists of several modules, i.e. image acquisition, preprocessing, segmentation, normalization, feature extraction, and matching. Figure 2 shows a flowchart of the designed iris recognition system.

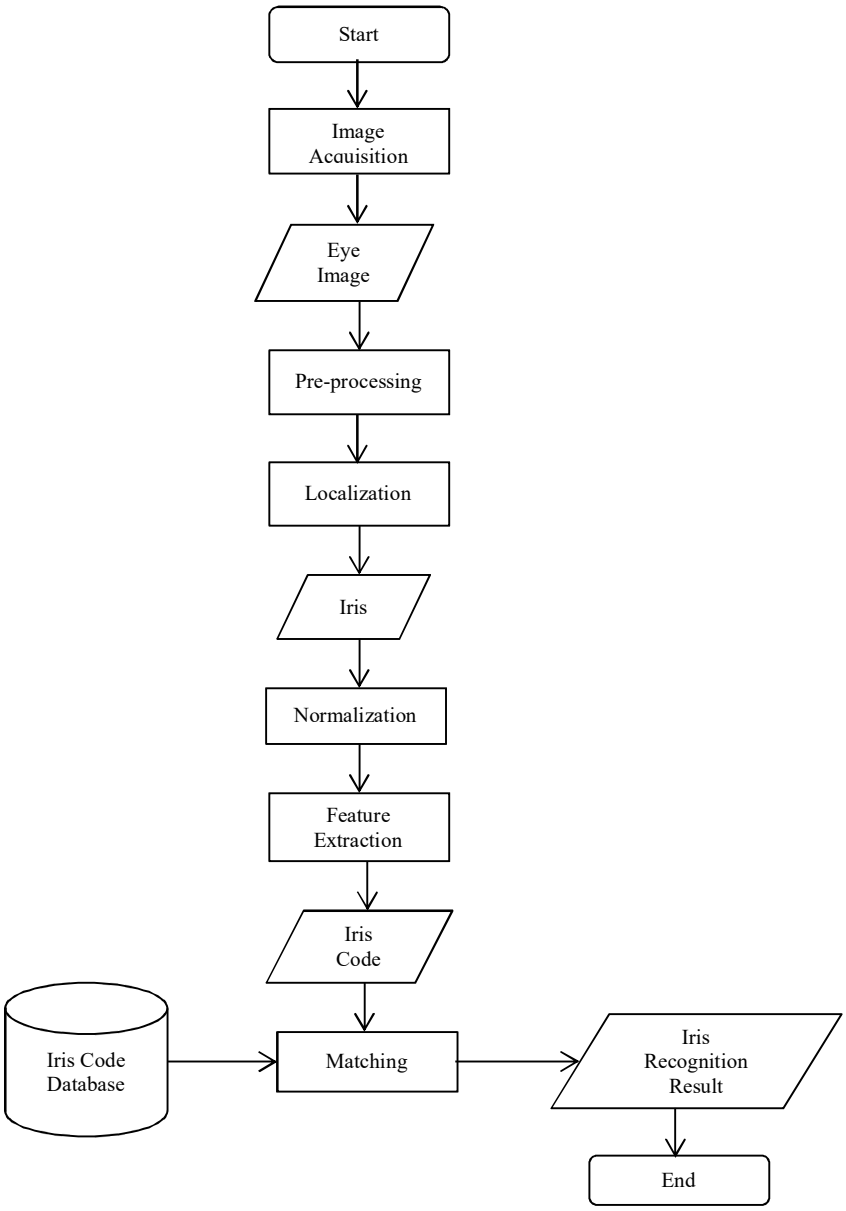

Figure 2 Flowchart of the proposed iris recognition system.

As shown in Figure 2, in the iris recognition process, first the iris image is acquired and pre-processing techniques are applied to improve the image quality. After that, the iris and pupil are localized (finding the area of the pupil and iris), segmented (the pupil and the iris areas are separated from other parts

of the eye), and normalized (the size of the iris is standardized). Subsequently, an iris code is generated from the normalized iris. This iris code is then used for the matching process.

3.3 Iris Segmentation using Gradient Magnitude and Fourier Descriptor

The proposed segmentation module uses the same technique as the one developed by Sentanoe [3] with some rule-based improvements, especially in the initial point localization step. Figure 3 shows the detailed process of iris segmentation using the conditional dilation technique with gradient magnitude calculation.

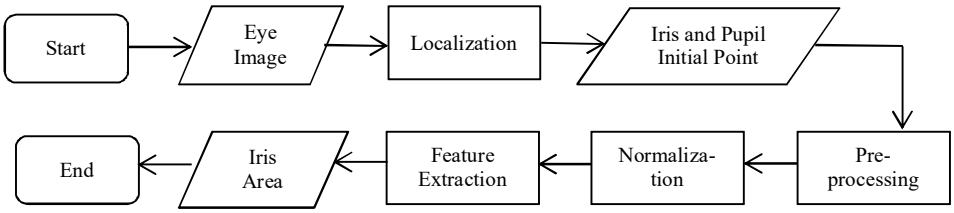

Figure 3 Iris segmentation using gradient magnitude with conditional dilation.

Eq. (1) represents the formula that is used to calculate the gradient magnitude and Eq. (2) describes the Fourier descriptor algorithm that is used in the boundary extraction step.

$$|G| = \sqrt{Gx^2 + Gy^2} \tag{1}$$

$$s(k) = \frac{1}{N}\sum_{u=0}^{M} a(u)e^{\frac{j2\pi ux}{N}} \tag{2}$$

where $|G|$ is the gradient magnitude, Gx represents the x-direction gradient, Gy represents the y-direction gradient, $s(k)$ is the sequence coordinate and $a(u)$ is the discrete Fourier transform.

3.4 Initial Point Localization

Figure 4 shows examples of inaccurate pupil and iris initial point localization by Sentanoe's iris segmentation module [3]. As can be seen in the right image of Figure 4, the iris's initial point was placed in the pupil area. The misplacement of the initial points usually occurs because of noise, varying pupil and iris size, and brightness. This may lead to failure in the conditional dilation step.

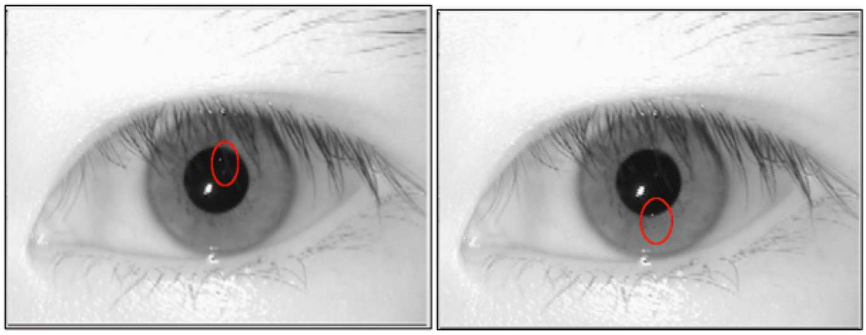

Figure 4 Example of inaccurate pupil and iris initial point localization. The red circle in the left image shows the pupil's initial point and the red circle in the right image shows the iris's initial point.

The pupil and iris initial points are the center coordinates of the pupil and the iris. In order to estimate the pupil's center coordinate, the proposed method uses the same techniques as Sentanoe [3], which are horizontal and vertical projection techniques as described by Eqs. (3) and (4). These techniques aim to find the darkest or brightest area in an image.

$$T(x) = \sum_{k=0}^{W} I(x,k)\text{n} \tag{3}$$

$$T(y) = \sum_{k=0}^{H} I(k,y) \tag{4}$$

where $T(x)$ is the total intensity of the image in the vertical direction, $T(y)$ is the total intensity of the image in the horizontal direction, and I represents the intensity level.

To find the iris's initial point, the pupil's center coordinate, which is obtained from Eqs. (3) and (4), is dilated by using the conditional dilation technique. This process is used to find the area of the pupil. Then, after the area of the pupil is obtained, the diameter of the pupil, the minimum coordinate of the pupil, the maximum coordinate of the pupil, and the exact center of the pupil can be calculated.

Eq. (5) represents the formula for calculating the accurate center coordinate of the pupil and Eq. (6) shows how to calculate the center coordinate of the iris.

$$C_p(x,y) = \frac{(\min\ (X_{P_i}) + \max\ (X_{P_i}))}{2}, \frac{(\min(Y_{P_i}) + \max\ (Y_{P_i}))}{2} \tag{5}$$

$$C_I(x,y) = C_P(x), (C_P(y) + \frac{d_p}{2} + 11) \tag{6}$$

where d_p is the pupil diameter, X_{P_i} and Y_{P_i} are collections of the pupil's x and y coordinates. The pupil diameter can be obtained by using Eq. (7).

$$d_P = \max\ (X_{P_i}) - \min\ (X_{P_i}) \tag{7}$$

Finding the accurate pupil's and iris's center coordinate is not the only significant aspect. Other factors, like the texture of the iris, the combination of high and low intensity in the iris and other dark areas in the image also play a role in causing failure in the conditional dilation step (see Figures 5 and 6). This is why, after the pupil's and iris's initial points have been obtained, the next step is to check whether the initial point can be dilated or not. If the iris's and pupil's initial points can be dilated, then the method will directly go to the next step, which is conditional dilation. However, if they cannot be dilated, the initial points will be shifted to the left, right, top or bottom until they can be dilated.

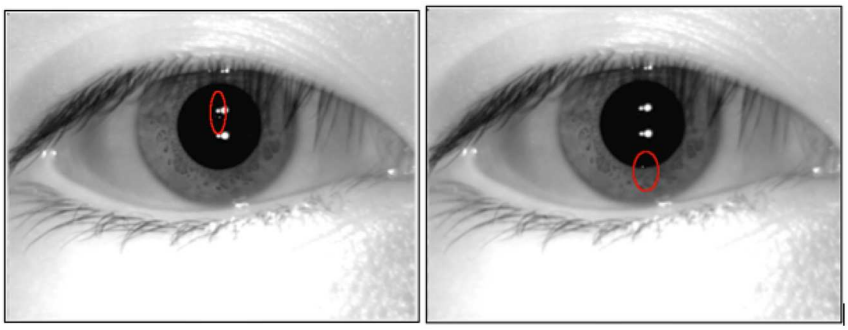

Figure 5 Example of misplaced pupil's (left) and iris's (right) initial point due to uncommon pupil size.

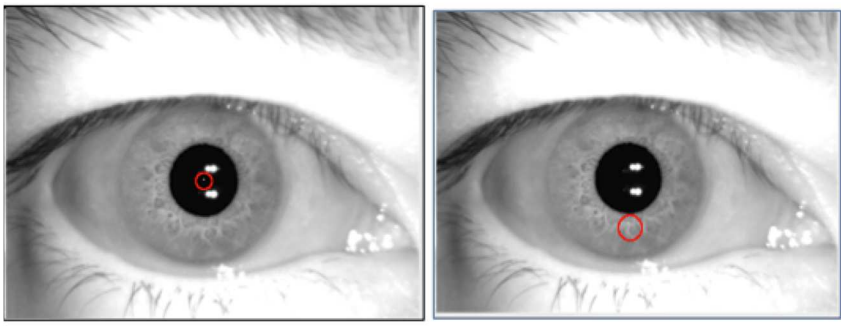

Figure 6 Example of iris initial point located in a high intensity area. The red circle in the left image represents the pupil's initial point and the red circle in the right image represents the iris's initial point, which is located in a higher intensity area compared to its neighborhood.

3.5 Conditional Dilation

In order to obtain the area of the pupil and the iris, the Sobel Edge Detector Algorithm is used. Eq. (8) represents the Sobel convolution mask for the x-axis and Eq. (9) is for the y-axis.

$$Gx = \begin{vmatrix} -1 & -2 & -1 \\ 0 & 0 & 0 \\ 1 & 2 & 1 \end{vmatrix} * (image) \tag{8}$$

$$Gy = \begin{vmatrix} -1 & 0 & 1 \\ -2 & 0 & 2 \\ -1 & 0 & 1 \end{vmatrix} * (image) \tag{9}$$

There are two parameters that affect the conditional dilation step, i.e. the threshold value and the number of iterations. The threshold value is used to decide whether the initial point can be dilated or not. Then, the number of iterations specifies how many times the gradient magnitude calculation needs to be done. These two parameters are acquired by using a parameter-tuning technique.

In our previous research [3], the number of thresholds was set to 45 and the number of iterations was set to 160. In this study, however, the threshold value was divided into two components, i.e. the threshold value for the pupil and the threshold value for the iris. The threshold value for the pupil was set to 20 and the threshold value for the iris was set to 45. This aims to solve problems with noise in the pupil area, as shown in Figure 7.

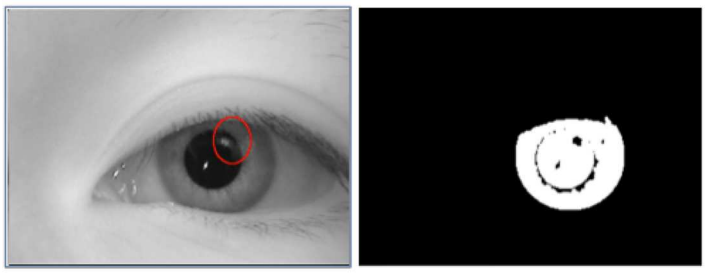

Figure 7 The left image shows the original eye image and the right image shows the pupil area.

3.6 Multimodal Biometrics Fusion using Neymann Pearson Algorithm

To fuse the matching score from the iris recognition system with the fingerprint recognition system, the Neymann Pearson algorithm was used. In the Neyman Pearson algorithm, to decide whether a person is accepted, Eq. (10) is used.

$$X \rightarrow match\ if\ \frac{p(S_1,S_2 \mid W_{genuine})}{p(S_1,S_2 \mid W_{impostor})} \geq \eta \tag{10}$$

where S_1 represents the matching score from iris recognition, S_2 represents the matching score from fingerprint recognition, and η represents the false matching rate that needs to be achieved for $W_{genuine}$ and $W_{impostor}$, as defined by Eqs.(11) and (12).

$$p(S_i \mid W_{genuine}) = \frac{1}{\sqrt{2\pi\sigma_{i,genuine}^2}}\, e^{\frac{-(S_i-\mu_{i,genuine})^2}{2\sigma_{i,genuine}^2}} \tag{11}$$

$$p(S_i \mid W_{impostor}) = \frac{1}{\sqrt{2\pi\sigma_{i,impostor}^2}}\, e^{\frac{-(S_i-\mu_{i,impostor})^2}{2\sigma_{i,impostor}^2}} \tag{12}$$

where σ_i represents the standard deviation for biometrics aspect i, and μ_i represents the mean for biometrics aspect i.

In this research, the values of σ_i and μ_i were derived from statistics of matching scores, which are shown in Table 1 below.

Table 1 Statistics of matching score.

	Genuine fingerprint matching score	**Impostor fingerprint matching score**	**Genuine iris matching score**	**Impostor iris matching score**
Number of samples	100	100	100	100
Mean (μ)	137	15	74	70
Standard deviation (σ)	47	3	3	1

Therefore, Eq. (10) can be derived into Eq. (13):

$$X \rightarrow match\ if\ \frac{\frac{1}{\sqrt{2\pi 3^2}} e^{\frac{-(S_i-74)^2}{2x3^2}}\ x\ \frac{1}{\sqrt{2\pi 47^2}} e^{\frac{-(S_i-137)^2}{2x47^2}}}{\frac{1}{\sqrt{2\pi 1^2}} e^{\frac{-(S_i-70)^2}{2x1^2}}\ x\ \frac{1}{\sqrt{2\pi 3^2}} e^{\frac{-(S_i-15)^2}{2x3^2}}} \geq \eta \tag{13}$$

4 Experimental Results

The accuracy of the iris recognition module in the proposed system is divided into three components: geodesic active contour step success, segmentation

success, and matching success. Table 4.1 describes the success rate for the three components.

Table 2 Iris recognition result overview.

Description	Success Rate
Geodesic active contour step	42.3%
Segmentation	97.4%
Matching	97.3%

Geodesic active contour step success means that the gradient magnitude calculation or the conditional dilation step was successful. This is determined by the following conditions:

1. Noise was successfully excluded in the conditional dilation process.
2. The sclera area was successfully removed during the conditional dilation step.

Figure 8 shows an example of geodesic active contour step success and failure.

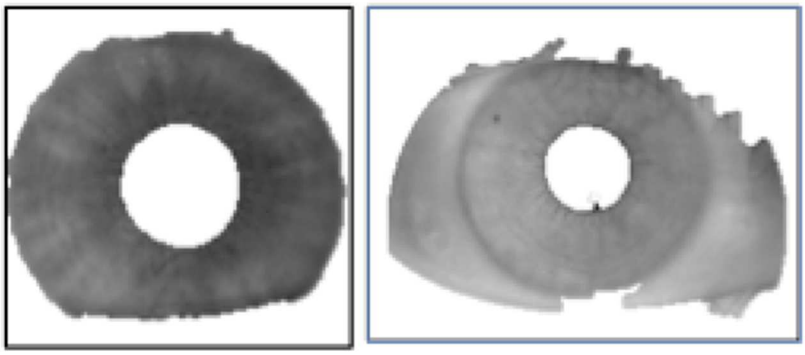

Figure 8 Geodesic active contour step success (left) and failure (right).

For segmentation, an iris is considered as successfully segmented when it fulfills the following requirements:

1. The sclera area was successfully excluded during the normalization process.
2. The iris does not contain noise after being unwrapped.

Figure 9 shows an iris image that was not successful in the geodesic active contour step but was successfully segmented.

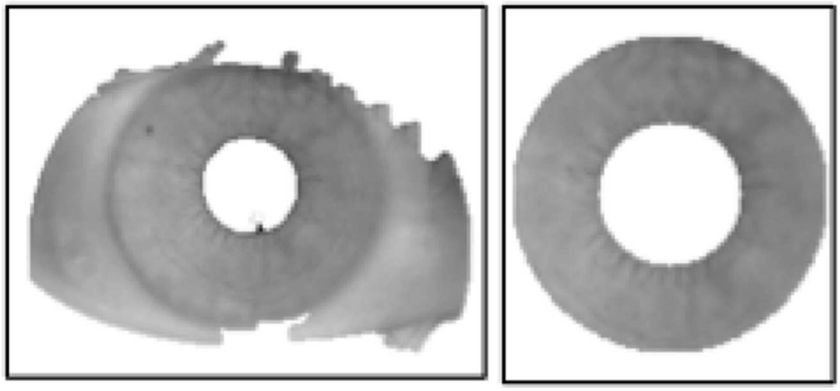

Figure 9 Conditional dilation result (left) and normalization result (right).

For the matching result, on the other hand, the matching step is considered successful when the hamming distance value of both the left and the right iris is lower than or equal to a certain threshold.

4.1 Segmentation Result

The proposed segmentation module was proven to be able to reduce the frequency of initial point misplacement. Figure 8 shows examples of initial points that were generated by the proposed system for the same eye image as the one that was used for obtaining the initial points in Figures 8 and 9 showing the result of the conditional dilation step.

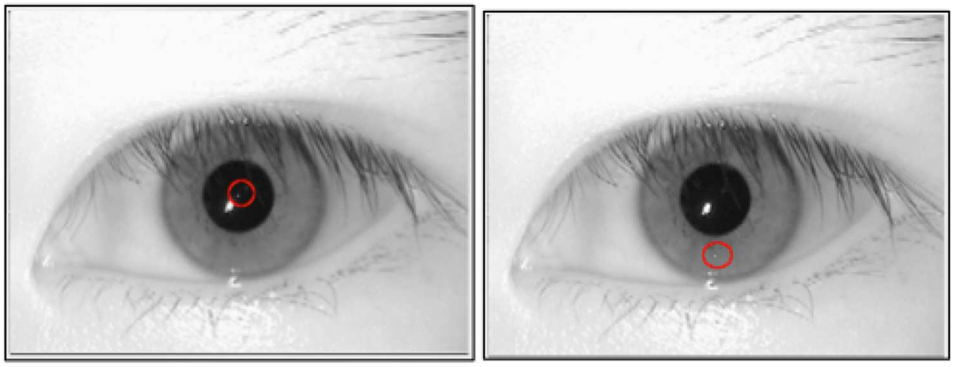

Figure 10 Pupil's (left) and iris's initial point (right) generated by the proposed segmentation module.

Figure 11 Result of conditional dilation step for initial points shown in Figure 10. The left image shows the pupil area that was obtained from the conditional dilation step and the right image shows the iris area that was acquired from the conditional dilation step.

As can be seen in Figure 11, the iris's initial point, which was initially located in the pupil area, was successfully fixed and shifted to the iris area. These accurate initial points lead to good results in the conditional dilation step.

In addition, the proposed segmentation module is also adequate in solving problems that are specified by Figure 7. Figure 12 shows an example of the conditional dilation step's result for the same eye image as the one that was used in Figure 7.

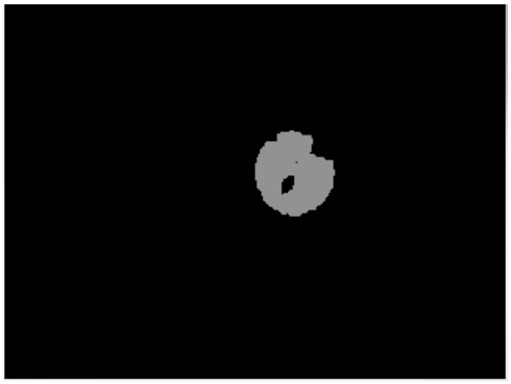

Figure 12 Result of conditional dilation step after applying median filter technique and separation of threshold value.

Table 3 shows a comparison of the segmentation module's accuracy rate between previous work [3] and the proposed module.

Table 3 Comparison of Sentanoe's [3] and proposed segmentation module accuracy results.

Description	Sentanoe [3]		Proposed System	
	Geodesic AC success rate	Segmentation success rate	Geodesic AC success rate	Segmentation success rate
MMUI database	20.4%	46.7%	44.4%	97.6%
SGU-MB-1 dataset	11.9%	59.5%	23.8%	95.2%
Overall result	19.7%	47.8%	42.7%	97.4%

Based on Table 3, the accuracy of the proposed iris segmentation module has increased approximately two times. The accuracy of the geodesic active contour algorithm is still low, but the overall segmentation result is quite satisfactory.

4.2 Accuracy of Proposed Iris Recognition System

To test the accuracy of the proposed iris recognition module, the Hamming distance algorithm was used.

Table 4 List of possible Threshold values and False Match Rates and False Non Match Rates.

Threshold	True Match (TM)	False Non Match (FNM)	False Match (FM)	True Non Match (TNM)	False Match Rate (FMR)	False Non-Match Rate (FNMR)
0.4	25	3	43	409	0.095	0.11
0.39	23	5	8	444	0.018	0.18
0.35	11	17	0	452	0	0.61

According to Table 4, the lowest false match rate (FMR) and false non-match rate (FNMR) were obtained by using 0.39 as the threshold value. Therefore, this research used 0.39 as the benchmark to decide whether the input and the template images belong to the same class.

Furthermore, Table 5 shows detailed testing results of the accuracy of the proposed iris recognition system.

Table 5 Detailed testing results of iris recognition matching module.

Descripti-on	True Match	False Non-Match	True Non-Match	False Match	False Match Rate	False Non-Match Rate	Matching Success Rate
MMUI database	16	4	374	6	0.015	0.2	97.5%
SGU-MB-1 dataset	7	1	70	2	0.03	0.14	96.3%
Overall result	23	5	444	8	0.018	0.18	97.3%

In Table 5, the matching success rate represents the probability of the system to reject an impostor and accept someone who is genuine.

4.3 Comparison between Single Biometrics and Multimodal

In order to test the multimodal attendence system, 90 pairs of irises and 90 fingerprints of the left point finger were used. Figures 13 until 15 show a comparison between the iris recogniton system, the fingerprint recognition system, and the multimodal fusion of both.

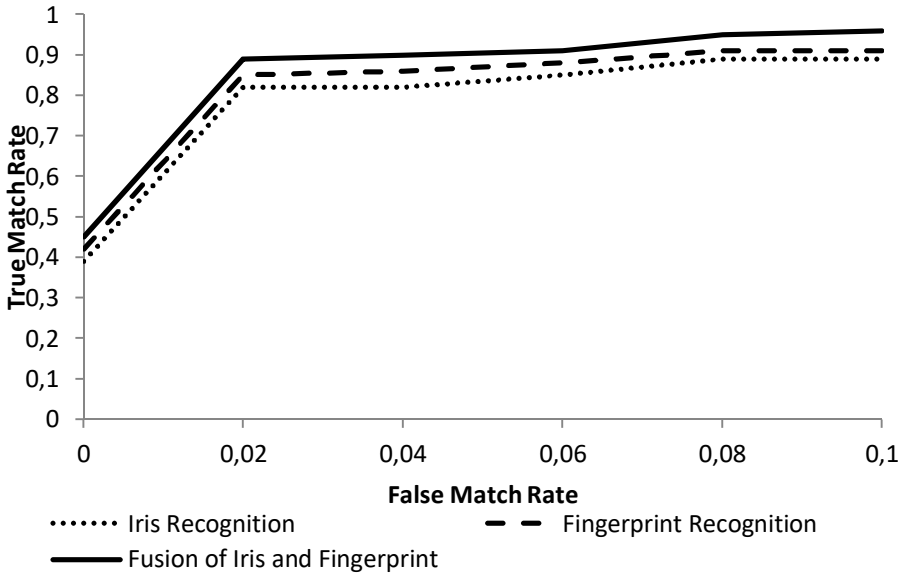

Figure 13 ROC graph for comparison of true match rate and false match rate between matchers.

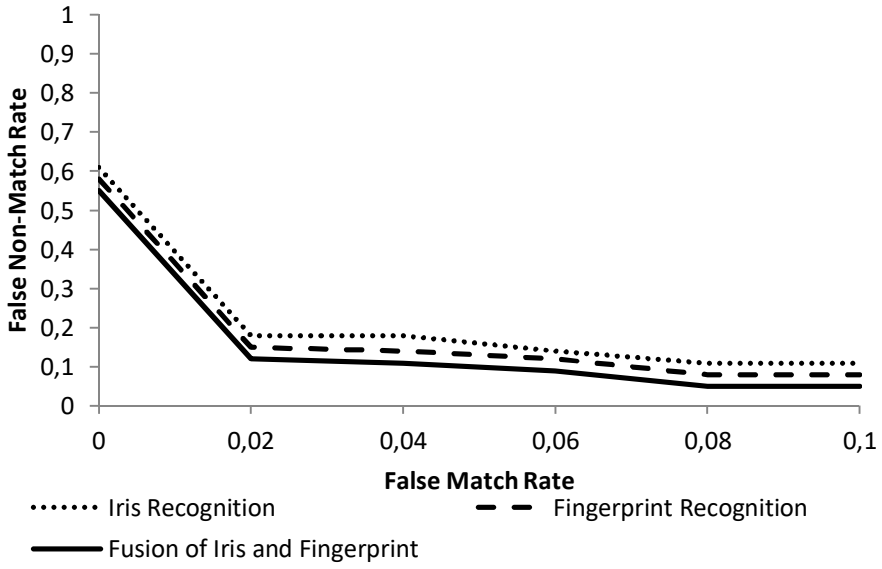

Figure 14 ROC graph for comparison of false non-match rate and false match rate between matchers.

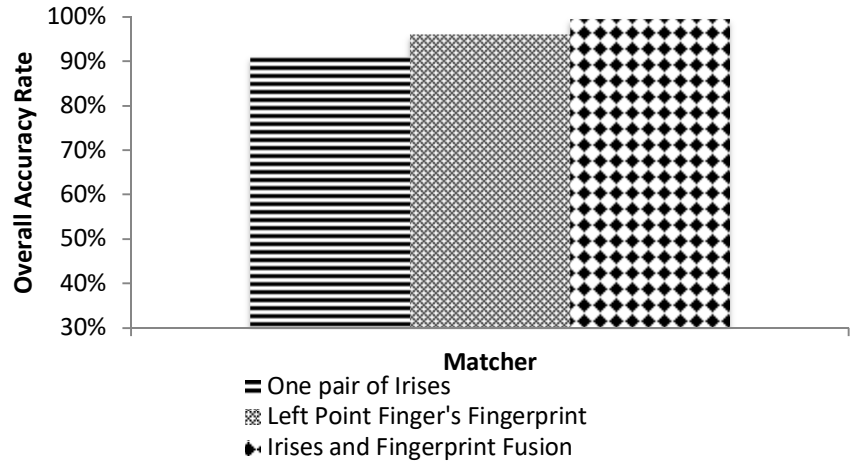

Figure 15 Comparison of overall accuracy rate between recognition of one pair of irises, fingerprint, and fusion of irises and fingerprint.

As can be seen in Figure 15 above, the accuracy rate of combining one pair of irises and one fingerprint was higher than the accuracy rate of the iris recognition system and fingerprint recognition system alone. Figure 16 shows a

graphic representation of the fusion score between the iris and the fingerprint recognition system.

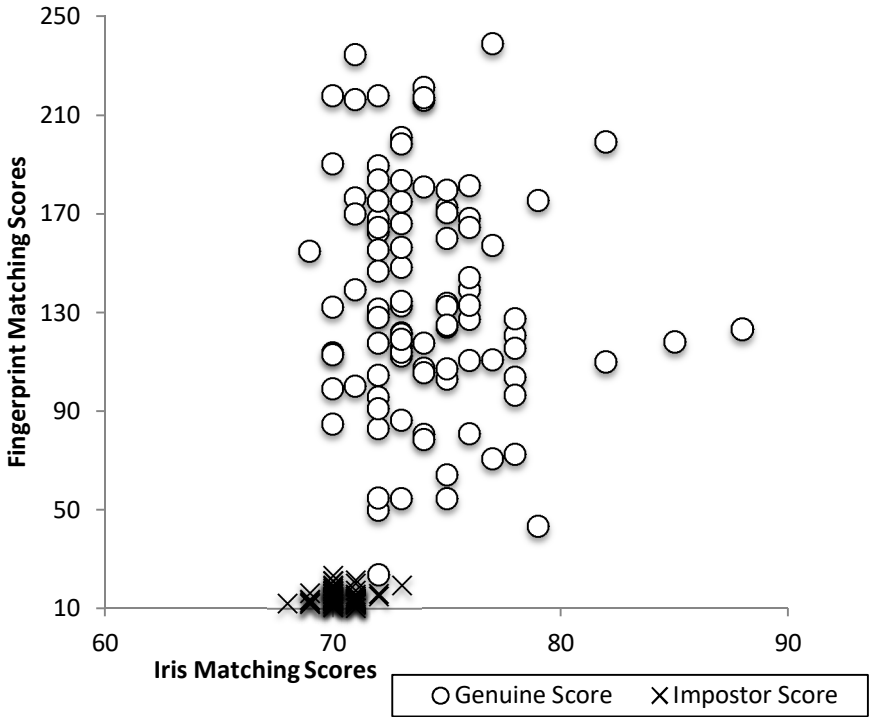

Figure 16 Fusion score of iris recognition system and fingerprint recognition system.

Both scores in the fusion graph in Figures 16 are based on similarities. That is why the larger the score is, the more similar the two irises or the fingerprints are. Since the result of the proposed iris recognition system is based on distance, the result needs to be converted using Eq. (14):

$$s = \frac{1}{1+HD} \tag{14}$$

where s represents the similarity score and HD represents the Hamming distance value.

5 Conclusions

Iris segmentation is one of most important steps in an iris recognition system. Failure in this step may lead to failure of the overall system. In order to improve the result of the previous work [3], the enhancements as explained in Section 3 were applied. Considering the experimental results, the accuracy rate of the

proposed segmentation module (97%) is quite satisfactory. However, improvements to the system's performance still need to be done. The advantage of the proposed iris segmentation algorithm compared to the integro-differential approach [4] is its the ability to deal with irregular iris contours, which are commonly found in most irides. This is similar to the goal of Ross and Shah's approach in [5], which evolves the iris contour until a predefined stopping criterion is achieved. Its accuracy notwithstanding, the evolution process in Ross and Shah's approach was computationally intensive. In contrast, our proposed method offers a simple algorithm based only on conditional dilation, thus requiring less computational effort and being suitable for real-time application. A comparison between this approach and Ross and Shah's approach in term of segmentation accuracy will be addressed in a follow-up to this study.

Regarding the results of this study, the best accuracy rate (almost 99%) was achieved by using the fusion between iris and fingerprint recognition, whereas the lowest accuracy rate (approximately 97%) was achieved using only the iris recognition system.

Acknowledgements

The author would like to thank the Swiss German University (SGU) for providing the opportunity to conduct and publish this research. Also, we would like to thank the Indonesian Agency for Assessment and Application of Technology as the facilitator of this research.

References

[1] Keekre, H.B. & Bharadi, V.A., *Ageing Adaptation for Multimodal Biometrics Using Adaptive Feature Set Update Algorithm*, Advance Computing Conference, 2009, IACC 2009, IEEE International, IEEE, 2009.

[2] Proenca, H. & Alexandre, L.A., *Toward Noncooperative Iris Recognition: A Classification Approach Using Multiple Signatures*. Pattern Analysis and Machine Intelligence, IEEE Transactions, **29**(4) pp. 607-612, 2007.

[3] Sentanoe, S., Nugroho, A.S., Galinium, M., Hartono, R. N., Uliniansyah, M.T. & Layooari, M., *Iris Localization using Gradient Magnitude and Fourier Descriptor,* in Proceedings of International Conference on Advanced Informatics: Concepts, Theory, and Application, Bandung, Indonesia, 2014.

[4] Daugman, J., *Probing the Uniqueness and Randomness of IrisCodes: Results from 200 Iris Pair Comparisons*, in Proceedings of the IEEE, **94**(11), pp. 1927-1935, 2006.

[5] Ross, A. & Shah, S., *Segmenting Non-Ideal Irises Using Geodesic Active Contours,* Biometrics Symposium: Special Session on Research at the Biometric Consortium Conference, IEEE Baltimore, Maryland, USA, 2006.

[6] Abhyankar, A. & Schuckers, S., *Active Shape Models for Effective Iris Segmentation,* Proceedings of SPIE The International Society for Optical Engineering, Defense and Security Symposium, Florida, USA, 2006.

[7] Valentina, C., Hartono, R.N., Tjahja, T.V. & Nugroho, A.S., *Iris Localization using Circular Hough Transform and Horizontal Projection Folding,* in Proceedings of International Conference of information Technology and Applied Mathematics Jakarta, Indonesia, pp. 64-68, 2012.